X International Conference on Computational Methods for Coupled Problems in Science and Engineering
COUPLED PROBLEMS 2023
M. Papadrakakis, B. Schrefler and E. Oñate (Eds)

HEMODYNAMIC EVALUATION OF AORTIC ANEURYSMS USING FSI SIMULATIONS

BHARGAV K. CHITNEEDI*,† AND CHRISTOS A. KARLIAMPAS*,‡

*Parallel CFD & Optimization Unit (PCOpt),
NTUA, Athens 15780, Greece
e-mail: bhargavchitneedi@mail.ntua.gr

†ESI Group,
3 Rue Saarinen, 94150 Rungis, France

‡Technevalue Group,
8808 Pfäffikon, Switzerland

Key words: Fluid-structure Interaction, Coupled Problems, Multi-physics Problems, Biomechanics

Abstract. The work focuses on understanding aortic blood flow dynamics and emphasize the importance of considering the flexible aortic wall model in assessing cardiovascular health and identifying potential risk factors for aneurysm and related conditions. In this paper, a fluid-structure interaction (FSI) study of vascular blood flow based on the partitioned approach using open-source software tools, OpenFOAM for Computational Fluid Dynamics (CFD) and CalculiX for Computational Structural Mechanics (CSM), coupled through the preCICE tool is presented. The FSI simulations were performed on raw and simplified (based on area of interest) patient-specific models of aneurysmatic blood vessels, considering Newtonian fluid and laminar flow assumptions. The arterial wall was modeled using the CalculiX's isotropic linear elastic model and the communication of data is handled by preCICE. The biomedical metrics such as the Time-Averaged Wall Shear Stress (TAWSS) and the Oscillatory Shear Index (OSI) in correlation with cardiac cycles were quantified to predict rupture prone regions.

1 INTRODUCTION

Understanding the dynamics of aortic blood flow is crucial for assessing cardiovascular health and identifying potential risk factors for diseases such as aneurysm, thrombosis etc. Aneurysms or abnormal bulges in blood vessels pose significant health risks and require comprehensive understanding for effective diagnosis and treatment. Aneurysms occur in various forms and locations, including abdominal aortic aneurysms, thoracic aortic aneurysms, and cerebral aneurysms [2]. Each type presents unique challenges due to their anatomical location, potential complications, and treatment options. The fatality rate increases significantly as the aneurysm leads to rupture. Thus, accurate diagnosis plays a crucial role in timely intervention and management [1].

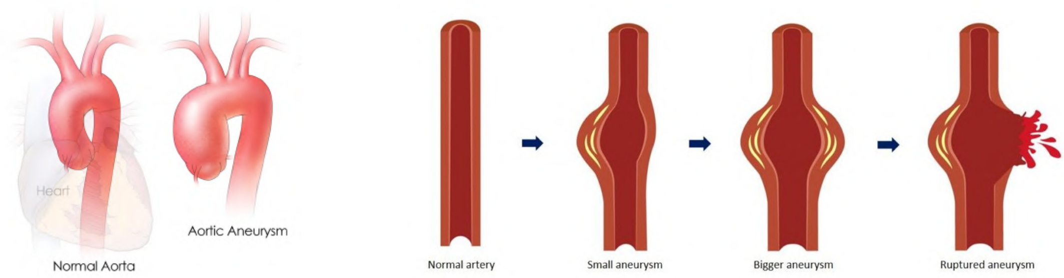

Figure 1: Aneurysm and it's progression to rupture [18][19]

Traditional diagnostic methods rely on imaging techniques such as ultrasound, computed tomography (CT) scans, magnetic resonance imaging (MRI), and angiography. While these methods offer insights into aneurysm presence and size, they are not without limitations. Radiation exposure in CT and MRI scans and the potential risk of complications associated with angiography necessitate alternative approaches. Additionally, detecting and monitoring small or complex aneurysms remains challenging using conventional techniques [3].

In the realm of applied mechanics, exploring the challenges associated with aneurysm diagnosis and leveraging simulation methods can provide valuable insights for improving patient care and outcomes. Simulation methods combining the merits of Computational Fluid Dynamics (CFD) and Computational Structural Mechanics (CSM) offer a promising path for enhancing the understanding of aneurysms. By modeling blood flow patterns, wall stress distribution, and rupture potential, simulations provide a non-invasive and cost-effective means to assess aneurysm behavior and guide treatment decisions [7]. These computational techniques empower researchers and medical professionals in the field of applied mechanics to contribute to advancements in aneurysm research and patient care.

However, performing accurate and reliable simulations for aneurysms has its own set of challenges because of the complex multi-physics phenomena involved. Ensuring an accurate representation of aneurysm geometries and physiological conditions requires robust imaging techniques and data processing. Selecting appropriate models for fluid-structure interaction, is crucial to accurately capture the dynamic behavior. Additionally, computational resources, including high-performance computing infrastructure, are necessary to handle the computational demands of simulations. Furthermore, validation of simulation results against clinical data and the establishment of standardized protocols for simulation-based diagnosis are essential for building trust in simulation approaches.

2 COMPUTATIONAL SPECIFICATIONS

The FSI problem of blood flow in aortic aneurysm is solved on unstructured grids based on the partitioned approach using opensource softwares; Openfoam [4] and CalculiX [5] coupled using the preCICE[6] coupling tool.

2.1 Flow solver

The unsteady incompressible Navier-Stokes equations govern the blood flow modeling in the aorta. For the fluid simulation, OpenFOAM which is based on Finite Volume Method is used. Among the available OpenFOAM solvers for incompressible flows, the pimpleFoam is selected due to its robustness in handling unsteady simulations and accommodating larger time steps, making it an ideal choice for our cases. To ensure the internal mesh conforms to the deformed wall mesh, a laplacian-based mesh morphing technique is employed.

2.2 Structural solver

For the structural simulations, the finite element method based CalculiX solver is employed. While shell elements could have been an ideal choice for this study, CalculiX, shell elements are automatically expanded into solid elements [5]. This approach may result in challenges, especially in regions with sharp corners and high curvature. To address this issue and ensure precise control over the initial mesh, 3D solid linear elements with uniform thickness to represent the aortic wall are generated.

2.3 Multi-physics Coupling

The partitioned FSI approach allows for the independent solution of the fluid and structural domains, efficiently handling the complex nature of the problem. It also allows easy replacement of one of the solvers without significant impact on the other solver. At the interface of both domains, data transfer and interpolation between the solvers are performed to enable accurate and stable simulations. In the current study, the open-source coupling library, preCICE [6], is used, which allows black-box coupling through adapters written for each solver which communicate with coupling tool. To reduce interpolation errors, matching interface meshes for both the fluid and structural domain is used. Implicit coupling method is used to avoid the added mass effect [10] and by using the quasi Newton acceleration scheme, efficiency is improved and robust convergence [8] is achieved.

2.4 Evaluation metrics

To assess the fluid forces exerted on the arterial wall and identify rupture-prone regions within the aneurysm, various hemodynamic indices were quantified to capture important features withing a cardiac cycle. This includes quantities based on wall shear stress (WSS) that are integrated over the cardiac cycle, like time-averaged WSS (TAWSS), and the Oscillatory Shear Index (OSI). The WSS is specifically evaluated at clinically crucial stages like systole during which the aortic valve is open and diastole is where aortic valve is closed. While the TAWSS gives temporal average the WSS magnitude distribution, the temporal mean WSS direction can be understood from OSI value[9]. In the below eq.2 the numerator is Averaged Wall Shear Stress Vector(AWSSV), which quantifies the mean shear vector[15].

$$TAWSS = \frac{1}{T}\int_0^T |\overrightarrow{\tau_w}| dt \tag{1}$$

$$OSI = \frac{1}{2}\left(1 - \frac{\left|\int_0^T \overrightarrow{\tau_w} dt\right|}{TAWSS}\right) \quad \text{, T is total time of cardiac cycle} \tag{2}$$

,

3 PATIENT SPECIFIC DATA & PRE-PROCESSING

Obtaining patient-specific medical data for fluid-structure interaction (FSI) simulations can be challenging due to various regulations and privacy concerns. The required data not only confines to geometric information but also corresponding essential parameters like flowrate, which are crucial for this study. Furthermore, the availability of suitable open-source data, particularly concerning aneurysms, is limited. To address these limitations, available data is acquired and meticulously tailored and pre-processed to suit the requirements of the current study. Focus was given on three relatively distinct cases, each obtained from open-source database [16][17].

3.1 Case 1 - Thoracic Aorta of a Healthy Patient

The thoracic aorta of a healthy patient with geometric and flowrate data was obtained from [16]. The surface mesh model, found to be suitable for the FSI simulations, was utilized without any further geometric pre-processing. In this case, the aortic model features one inlet and five outlets.

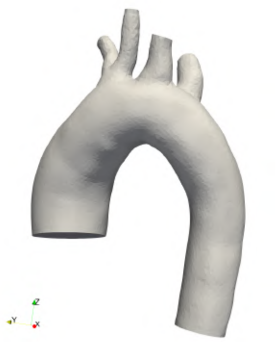

(a) Healthy thoracic aorta model

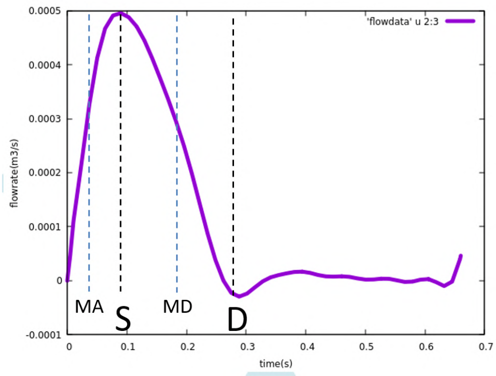

(b) Flowrate profile

Figure 2: Healthy thoracic aorta model and corresponding flowrate

3.2 Case 2 - Thoracic Aorta with Aneurysm

Patient-specific data for the thoracic aorta with an aneurysm was obtained from opensource database [16], combining geometric information and flowrate data. However, certain challenges arose during the solid mesh creation process due to the branched arteries of the ascending aortic arch being in close proximity (less than 4mm) at specific locations. This resulted in intersecting elements when attempting to generate a 2mm thick solid mesh. Such proximity might also lead to intersecting elements due to deformations, especially since a contact model was not utilized in this study. To overcome this issue, branches were removed and sealed, resulting in a simplified model with a single inlet and outlet configuration.

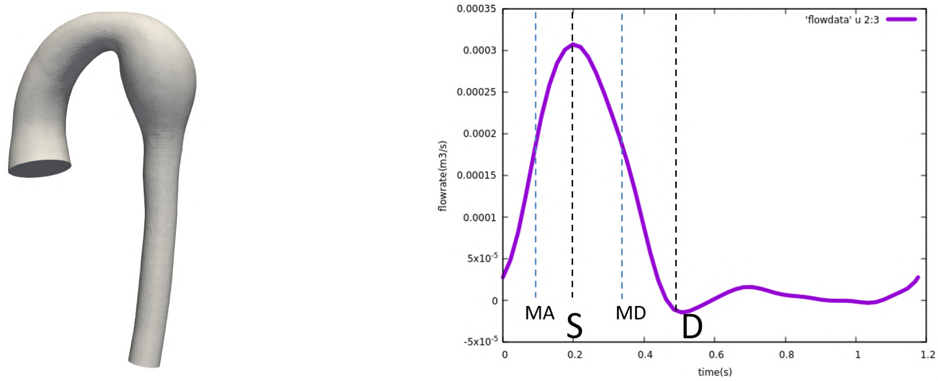

(a) Aneurysmatic thoracic aorta model (b) Flowrate profile

Figure 3: Thoracic aorta with aneurysm model and corresponding flowrate

3.3 Case 3 - Bifurcation Aorta

An additional model of a bifurcation artery, distinct from the other two cases, was obtained [17] without flowrate information. Given the study's emphasis on large arteries, the acquired carotid artery model was scaled to match the diameter of the abdominal aorta. To replicate the cardiac cycle, an idealized parabolic flow rate profile was created for this simulation.

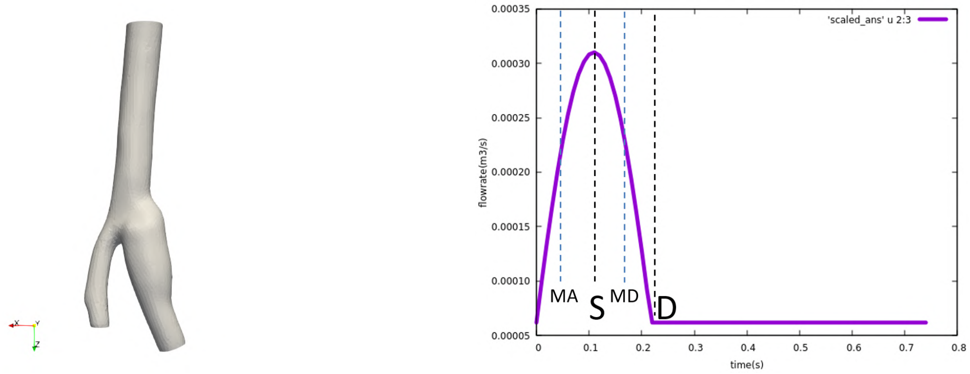

(a) Bifurcation aorta model (b) Flowrate profile

Figure 4: Bifurcation aorta model and corresponding flowrate

4 SIMULATION CONDITIONS

After undergoing geometric processing, all the acquired models are utilized to generate a hybrid unstructured boundary layer volume mesh, comprising of prisms and tetrahedra. Although blood exhibits non-Newtonian properties, in the context of large arteries like the aorta, the influence of non-Newtonian behavior is considered insignificant. Thus, for the present study of aortic blood flow, we assume a constant viscosity. To represent the cardiac cycle, the patient-specific geometry along with the corresponding flowrate profile is acquired. Given the periodic nature of cardiac cycles, extending the simulation for multiple cycles ensures a smooth and well-converged analysis. Unsteadiness is induced at the inlet through a time-varying volumetric flowrate profile that corresponds to the cardiac cycle, while the spatial profile is assumed to be uniform.

The aortic wall exhibits complex non-linear structural properties due to its biological nature. Although an anisotropic hyperplastic model would provide the closest approximation, obtaining in-vivo mechanical properties for patient-specific models is challenging. Therefore, for computational efficiency and simplicity, an isotropic linear model to represent the aortic wall is chosen. Additionally, a uniform thickness for the aorta is assumed due to the lack of thickness information from medical image data.

4.1 Boundary conditions

For the fluid solver, the pulsatile flow-rate profile is imposed at inlet corresponding to the cardiac cycle, while the spatial profile is assumed to be uniform. At the outlets, zero-pressure is imposed. To ensure no slip condition while the wall moves along the deformation vector, moving wall velocity boundary condition is imposed on the wall. On the other hand, for the structural solver, inlet and outlets are constrained by applying zero displacement Dirichlet boundary condition. The concentrated loads are applied at the wall nodes which are derived from the fluid forces during the interaction data exchange.

4.2 Material properties

The fluid properties are assigned to mimic the characteristics of blood with the density of 1060 kg/m3 and the kinematic viscosity of 3.5e-6 m2/s. For the structural simulations, the aortic vessel is represented with uniform thickness of 2mm, density of 1200 kg/m3, Poisson ratio of 0.45, and the Young's modulus of 1.1e6 Pa [7].

5 RESULTS AND DISCUSSION

The three cases described in previous sections have different set of challenges to achieve a stable converged solution. The bifurcation aorta case has smooth flow rate profile with positive values all over. On the other hand, the thoracic aorta cases had negative flow-rate at the inlet for a short period during diastole. The simulations were destabilised while the inlet behaves as outlet. In such cases, to approximate convective fluxes, Gauss Upwind divergence scheme of openFOAM performs better in handling steep variations in flow features but the computational efficiency reduces. For simpler cases Gauss Linear Upwind scheme would be sufficient. Among the coupling schemes available in preCICE, the quasi Newton schemes performed better than Dynamic Aitken under-relaxation. The IQN-IMVJ scheme was used for all the simulations.

The time evolution of the WSS is evaluated at mid-acceleration(MA), systole(SYS), mid-deceleration(MD), diastole(DIAS) stages of cardiac cycle. The time integrated quantities TAWSS and OSI were computed for one cardiac cycle and analysed. However, it is essential to note that while these metrics provide understanding about major flow components, they cannot directly predict vessel rupture. The issue is complex, involving biological tissues that respond and adapt to their conditions, leading to tissue remodeling. While both high and low WSS can lead to aneurysm growth progression the combination of low TAWSS and high OSI is high likely to cause aneurysm rupture[14].

5.1 Case 1

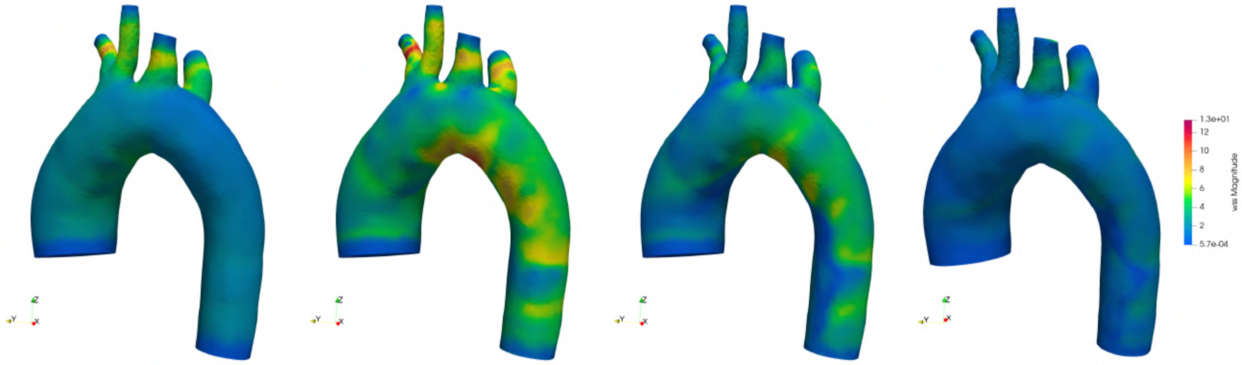

(a) WSS (MA) (b) WSS (Systole) (c) WSS (MD) (d) WSS (Diastole)

Figure 5: Healthy Aorta: WSS at different stages of cardiac cycle

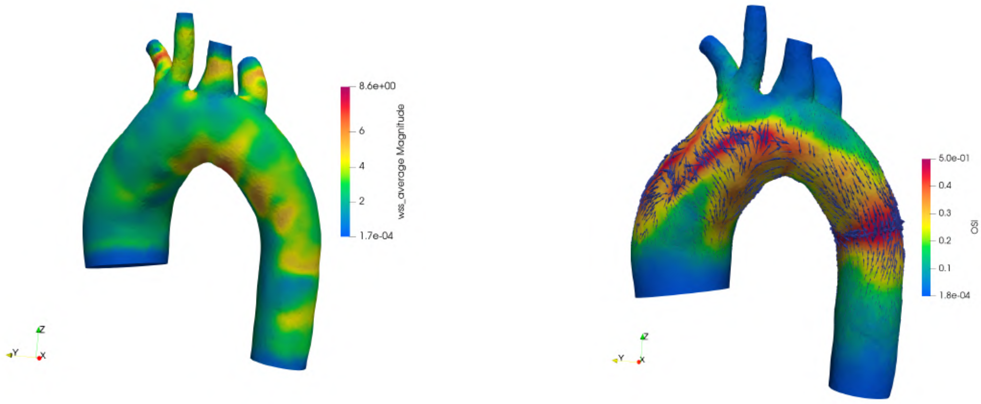

(a) TAWSS (b) OSI

Figure 6: Healthy Aorta: TAWSS and OSI

From the figure 5, during systole, WSS values are considerably higher than other stages unlike case 1 where systole and MD were crucial. In this case, the inner radius of aortic arch has higher WSS values. Due to the constraints imposed at the inlet and the four outlets the displacement of the aorta is very restricted compared to case 1.

Figure 6(a) shows the TAWSS distribution which resembles WSS distribution at systole but with pronounced gradients. In the figure 6(b) the OSI gradients are very high suggesting violent flow close to the wall. The AWSSV concentration at the higher gradients is evidently seen.

5.2 Case 2

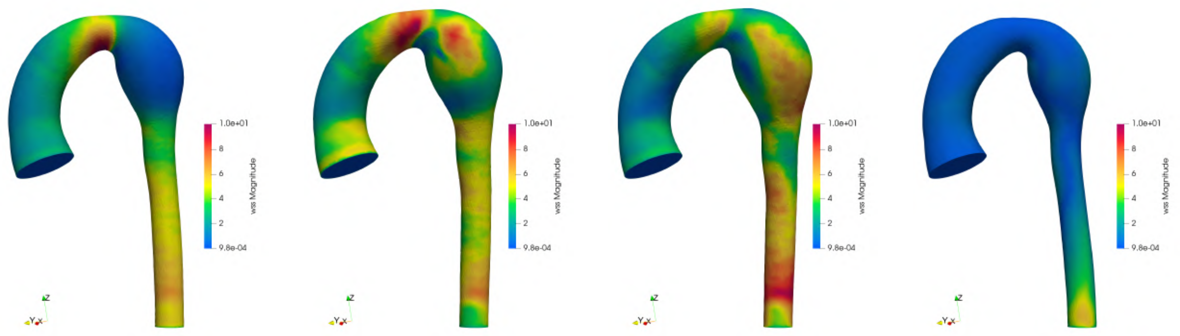

(a) WSS (MA) (b) WSS (Systole) (c) WSS (MD) (d) WSS (Diastole)

Figure 7: Aneurysmatic thoracic aorta: WSS at different stages of cardiac cycle

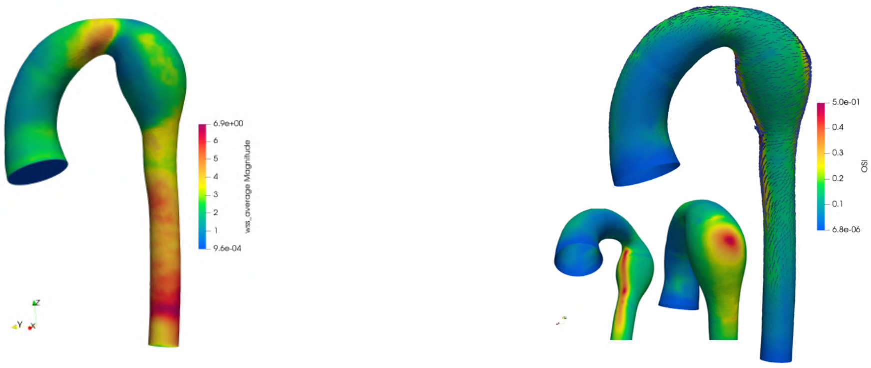

(a) TAWSS (b) OSI

Figure 8: Aneurysmatic thoracic aorta: TAWSS and OSI

The figure 7 illustrates WSS distribution at crucial stages of cardiac cycle. During systole, the WSS values are notably high near the aneurysm neck, accompanied by high contour gradients indicating flow recirculation with sharp gradients. Between the MA and MD stages, it shows that flow field is very dynamic during MD, resulting in higher WSS values. The aneurysm bulge expands considerably larger than other regions, with the maximum diameter observed at the MD stage. Comparing the diameters of the aneurysm bulge and ascending aorta, we find that both experience notable increases during systole and MD stages. The center of the aneurysm bulge diameter increases by 14.4% and 17.6% during systole and MD stages, respectively, while the ascending aorta diameter increases by 8.5% and 10.1% during the same stages.

Figure 8(a) displays the time-averaged wall shear stress (TAWSS), computed by integrating WSS magnitude over the cardiac cycle, indicating higher gradients near the aneurysm neck region. To gain insights into the mean shear direction, we use the averaged wall shear stress vector (AWSSV) plotted on the OSI value in Figure 8(b). The inner and outer radius of the aortic arch exhibits higher OSI concentration, signifying greater WSS gradients within these regions over one cardiac cycle.

5.3 Case 3

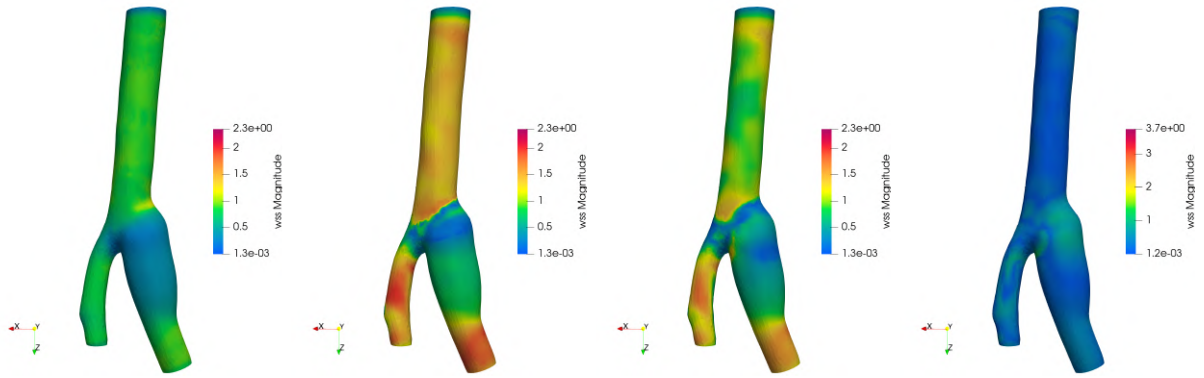

(a) WSS (MA) (b) WSS (Systole) (c) WSS (MD) (d) WSS (Diastole)

Figure 9: Bifurcation aorta: WSS at different stages of cardiac cycle

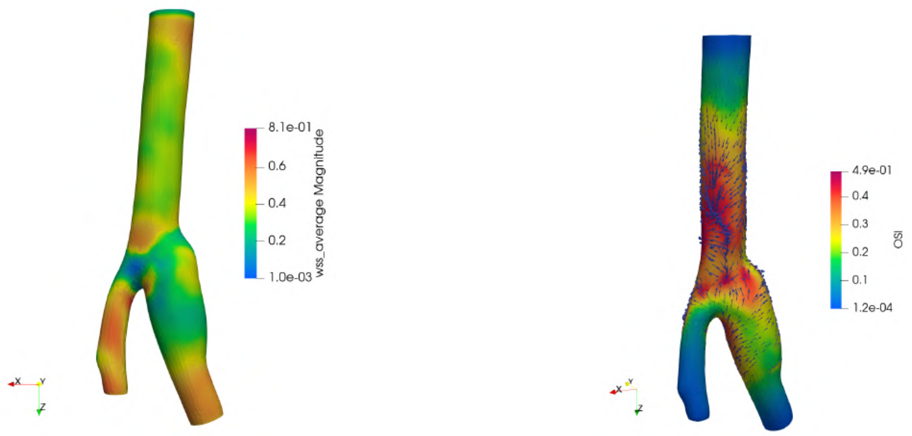

(a) TAWSS (b) OSI

Figure 10: Bifurcation aorta: TAWSS and OSI

From the figure 9, both systole and MD stages has concentrated WSS distribution. Especially during systole these is almost discontinuous WSS distribution near the bifurcation. The branch which bulges resembling the aneurysm has lower WSS values compared to other branch. The figure 10(a) shows the TAWSS distribution relatively smoother except near the bifurcation junction. The OSI plot in figure. 10(b) still shows some concentrations right before the bifurcation because of disturbed flow before the bifurcation.

6 CONCLUSIONS

The study explores the feasibility of FSI simulations for hemodynamics using Open Source libraries and tools in a HPC environment. Three distinct cases (smooth aneurysmatic thoracic aorta, healthy thoracic aorta, abdominal aorta) were investigated with special focus to quantify WSS (instantaneous and time-averaged), OSI metrics which are correlated to TAWSS with higher rupture risk. Results show in general a concentration of high WSS during systole and around the aneurysm (or enlargements of the aortas) neck. Aneurysmatic areas exhibiting also high values of AWSSV gradient can be susceptible to tearing and should be considered for monitoring by clinicians and treatment in later stages. Overcoming challenges such as accurate geometry representation, model selection, computational resources, and validation will pave the way for personalized medicine and improved management of aneurysms. Continued research and collaboration among applied mechanics experts, and medical professionals will advance the field, ultimately leading to better diagnostic methods and treatment strategies for aneurysm patients.

7 ACKNOWLEDGEMENTS

The work has received funding from the European Union's Horizon 2020 research and innovation programme under the Marie Skłodowska-Curie grant agreement No 859836, MeDiTATe: "The Medical Digital Twin for Aneurysm Prevention and Treatment". All authors approved the version of the manuscript to be published. The authors wish to thank Professor Kyriakos Giannakoglou, NTUA for supervising this work.

REFERENCES

[1] https://www.health.harvard.edu/heart-health/shining-a-light-on-thoracic-aortic-disease

[2] https://www.webmd.com/heart-disease/heart-disease-aortic-aneurysm

[3] L. Hacein-Bey, JM. Provenzale, "Current imaging assessment and treatment of intracranial aneurysms", American Journal of Roentgenology, Volume 196,1, 2011

[4] OpenFOAM project web pages. http://www.openfoam.org (2004).

[5] G. Dhondt. "Calculix crunchix user's manual version 2.12.", 2017.

[6] HJ. Bungartz et al. "preCICE – A fully parallel library for multi-physics surface coupling", Computers & Fluids, Volume 14, 2016

[7] A. Mourato et al. "Computational Modelling and Simulation of Fluid Structure Interaction in Aortic Aneurysms: A Systematic Review and Discussion of the Clinical Potential", Applied Sciences, Volume 12, 2022

[8] A.E.J. Bogaers, S. Kok, B.D. Reddy, T. Franz, "An evaluation of quasi-Newton methods for application to FSI problems involving free surface flow and solid body contact", Computers & Structures, Volume 173, 2016

[9] R. Amaya, LM. Cancel, JM. Tarbell, "Interaction between the Stress Phase Angle (SPA) and the Oscillatory Shear Index (OSI) Affects Endothelial Cell Gene Expression". PLoS One, Volume 11, 2016

[10] P. Causin, J.F. Gerbeau, F. Nobile, "Added-mass effect in the design of partitioned algorithms for fluid–structure problems", Computer Methods in Applied Mechanics and Engineering, Volume 194, 2005

[11] M.L. Cerquaglia, D. Thomas, R. Boman, V. Terrapon, J.-P. Ponthot, "A fully partitioned Lagrangian framework for FSI problems characterized by free surfaces, large solid deformations and displacements, and strong added-mass effects", Computer Methods in Applied Mechanics and Engineering, Volume 348, 2019

[12] ST. Ha, HG. Choi, "Investigation on the effect of density ratio on the convergence behavior of partitioned method for fluid–structure interaction simulation", Journal of Fluids and Structures, Volume 96, 2020

[13] E. Vignali, E. Gasparotti, S. Celi and S. Avril, "Fully-Coupled FSI Computational Analyses in the Ascending Thoracic Aorta Using Patient-Specific Conditions and Anisotropic Material Properties", Frontiers in Physiology, Volume 12, 2021

[14] M. Boniforti, et al., "Image-Based Numerical Investigation in an Impending Abdominal Aneurysm Rupture", Fluids, Volume 7, 2022

[15] R. Campobasso, F. Condemi, M. Viallon et al., "Evaluation of Peak Wall Stress in an Ascending Thoracic Aortic Aneurysm Using FSI Simulations: Effects of Aortic Stiffness and Peripheral Resistance", Cardiovascular Engineering and Technology , Volume 9, 2018

[16] https://www.vascularmodel.com/

[17] https://grabcad.com/

[18] https://med.uth.edu/internalmedicine/medical-genetics/john-ritter-research-program/

[19] https://quantummed.sg/impressions-post/abdominal-aortic-aneurysm-taking-control-of-the-time-bomb/